IEEE Access
Multidisciplinary | Rapid Review | Open Access Journal

Received 17 June 2023, accepted 7 July 2023, date of publication 19 July 2023, date of current version 26 July 2023.

Digital Object Identifier 10.1109/ACCESS.2023.3296795

RESEARCH ARTICLE

Changes in Maritime Traffic Patterns According to Installation of Floating LiDAR Using Spatial Analysis

JEONG-SEOK LEE[1], MOON-SUK LEE[2], AND IK-SOON CHO[3]
[1]Graduate School, Korea Maritime and Ocean University, Busan 49112, South Korea
[2]Ocean Policy Research Center, Korea Institute of Ocean Science and Technology, Busan 49112, South Korea
[3]Division of Maritime AI and Cyber Security, Korea Maritime and Ocean University, Busan 49112, South Korea

Corresponding author: Ik-Soon Cho (ischo@kmou.ac.kr)

This work was supported by the Development of Simulation Technology for Maritime Spatial Policy by the Ministry of Oceans and Fisheries under Grant 20220431.

ABSTRACT Recently, with the development of marine space around the world, friction between maritime traffic and various marine activities is intensifying. In particular, different recommendations are being made for the buffer zone between offshore wind farms and maritime traffic, as the criteria vary significantly. In order to respond to these changes in marine space, conducted this study on the change of maritime traffic patterns before and after the installation of floating LiDAR (Light Detection And Ranging) in marine facilities and apply it to future changes in maritime traffic patterns. The maritime traffic data was based on Automatic Identification System (AIS) data, and it was targeted at cargo ships and tankers with regular traffic patterns. A trajectory and spatial analysis were performed based on the AIS in the marine space. As a result of analyzing the globally maritime traffic patterns targeting the location of the installation complex of LiDARs, it can be confirmed that the existing maritime traffic patterns change into three maritime traffic patterns. Furthermore, the study employed the Hausdorff-distance algorithm for clustering analysis, categorizing vessels with similar trajectories. This approach facilitated a locally analysis of the buffer zone associated with individual LiDAR, considering the length of the vessels. As a result, it was analyzed that each vessel navigated at different buffer zone depending on the size of the vessel, and it is possible for safe navigation and forecast the future maritime traffic patterns.

INDEX TERMS Maritime traffic, marine facilities, automatic identification system (AIS), spatial analysis, buffer zone.

I. INTRODUCTION

The shipping industry is the most effective way to use the space of the sea and transport cargo over long distances [1]. 99.7% of Korea's import and export volume is transported through ships, which constitute a major cargo [2]. Accordingly, ships operating in the coastal waters of Korea maintain the customary traffic patterns, and most ships show similar routes [3]. In addition, as the shipping industry continues to develop and the demand for maritime transportation increases, the size of ships has increased [4]. In accordance with these circumstances, world organizations or national levels are recommending the establishment of routes and the separation distance from marine facilities for the safe operation of ships and the prevention of marine accidents. In particular, Article 60 of the UN (United Nations) Maritime Act suggested the safe separation distance between ships and marine facilities in the beta economic zone as 500m [5]. In PIANC (The World Association for Waterborne Transport Infrastructure) WG 161, the width of the patterns for offshore wind farms and passing vessels is determined based on TSS (Traffic Separation Scheme) or the end of the set route [6]. In the UK, 90% of traffic patterns is selected and set as a spare water area to set a safe separation distance for wind farms and passing ships [7]. The values of the various separation distances or safety zone settings presented above represent the results considering only the maritime traffic or the ship's maneuvering performance. That is calculation method that

The associate editor coordinating the review of this manuscript and approving it for publication was Tao Wang.

does not consider the change value after the installation of marine facilities. Therefore, it is necessary to analyze the patterns of maritime traffic that changes according to the installation of floating LiDAR (Light Detection And Ranging) in marine facilities and set the separation distance and safe water area based on this.

On the other hand, according to the recent active progress of marine spatial planning, marine space is classified spatially and temporally and the marine environment and safety are preserved [8], [9], [10]. In particular, friction between maritime traffic and offshore wind farms in the marine space is intensifying. In order to respond to the increasingly complex maritime space, preemptively securing space for maritime traffic and analyzing conflicting sea areas with marine facilities [11]. The purpose of this study is to predict changes in maritime traffic patterns in the future maritime space depending on the presence or absence of maritime facilities. Analysis of changes in maritime traffic patterns before and after installation targeting the sea area LiDAR for offshore wind generation are installed. In the case of Korea, the analysis area of this study, uncontrolled offshore wind farm development is planned for most coastal areas [12]. Prior to the installation of offshore wind farms, LiDAR is installed to measure wind resources and is observed for several years [13], [14]. Therefore, any facilities installed in the ocean unavoidable have an impact on maritime traffic and bring about changes in navigation patterns.

In order to perform efficient and quantitative analysis, a trajectory analysis is performed based on AIS (Automatic Identification System) data [15], [16]. The AIS data contains information on maritime traffic operations and is widely used for various analyses [17], [18], [19]. Here, the entire area where LiDARs are installed is spatially and globally analyzed to determine the overall change in maritime traffic patterns. The Hausdorff-distance algorithm is used to remove data such as outliers, abnormal tracks, and ship turning included in the track diagram analysis and display only similar tracks [20]. Similar tracks were clustered, and finally, the buffer zone distance for individual LiDARs were analyzed in detail locally [21], [22]. Recognizing changes in maritime traffic allows for analysis of conflicts in different marine activities, which can be applied to the marine digital twin to proactively identify areas with high levels of conflict and prevent potential issues [23], [24]. By analyzing the patterns of maritime traffic according to the installation of marine facilities, the purpose is to predict or apply future maritime traffic patterns changes. In addition, the change value of the actual maritime traffic patterns is used to prevent maritime accidents to contribute to the preservation of the marine environment.

II. METHODS

Maritime traffic patterns are created for safety and economic reasons over an extended period [25]. In other words, vessels tend to use routes that were predominantly used in the past, and they are significantly affected by the installation of marine facilities or offshore wind farms [26]. Particularly, predicting changes in vessel navigation patterns becomes more challenging as the installation area increases. Therefore, this study aims to quantify the changes in maritime traffic using spatial analysis, focusing on a location with 15 LiDAR devices installed. The research on maritime traffic pattern changes will help address the limitations of predictive simulations and determine a safe buffer zone depending on vessel characteristics. This offers a new perspective on calculating the buffer zone between offshore wind farms and maritime traffic, which differs from the approaches proposed by PIANC and the UK.

A. ANALYSIS DOMAIN MODELING

The analysis method for identifying changes in maritime traffic patterns according to the installation of floating LiDAR is shown in Figure 1. First, the analysis area is set and the corresponding AIS data is extracted. To extract AIS data, a total of 3 years of data from 2018 to 2021 stored in the database is utilized. This data has a capacity of approximately 1.5TB and is based on all AIS data from vessels that have navigated along the coast of South Korea.

This process includes cleaning and pre-processing of the data. AIS data is generally divided into static information and dynamic information [27]. Static information includes Maritime Mobile Service Identity (MMSI), name, type, IMO number, callsign, length, draft, and gross tons (GTs), while dynamic information includes MMSI, date, latitude, longitude, SOG, COG, and heading [28]. In this process, the dynamic data is combined with the static data, ensuring that the AIS data for the vessels can be used comprehensively and effectively [29]. Since the extraction of maritime traffic data is basically composed of point data, it is displayed as a track map by connecting it with a line [30]. To create a ship's trajectory, points logged over time can be linked by establishing a field group named MMSI, enabling the formation of the ship's trajectory line [31]. Next, the process involves modeling different layers of maritime spatial information necessary for analysis and encompasses mapping essential spatial analysis, aiming to discern alterations in global maritime traffic patterns. For conducting spatial analysis, the grid modeling was created with a 1km $\times$ 1km. After that, based on the analysis results of the data, it is a process of figuring out the overall patterns in the ocean area where the LiDAR area shows the form of integration. Then, a process of removing abnormal tracks, outliers, and irregular navigation patterns included in the ship trajectory map and clustering only similar trajectory is performed [32]. Here, the Hausdorff-distance algorithm is used and tracks of similar shape are clustered. The result of track clustering finally calculates the change in maritime traffic patterns in the local space centered on LiDAR. Therefore, the maritime traffic patterns in the future maritime space can be used to apply the change value according to the presence or absence of maritime facilities.

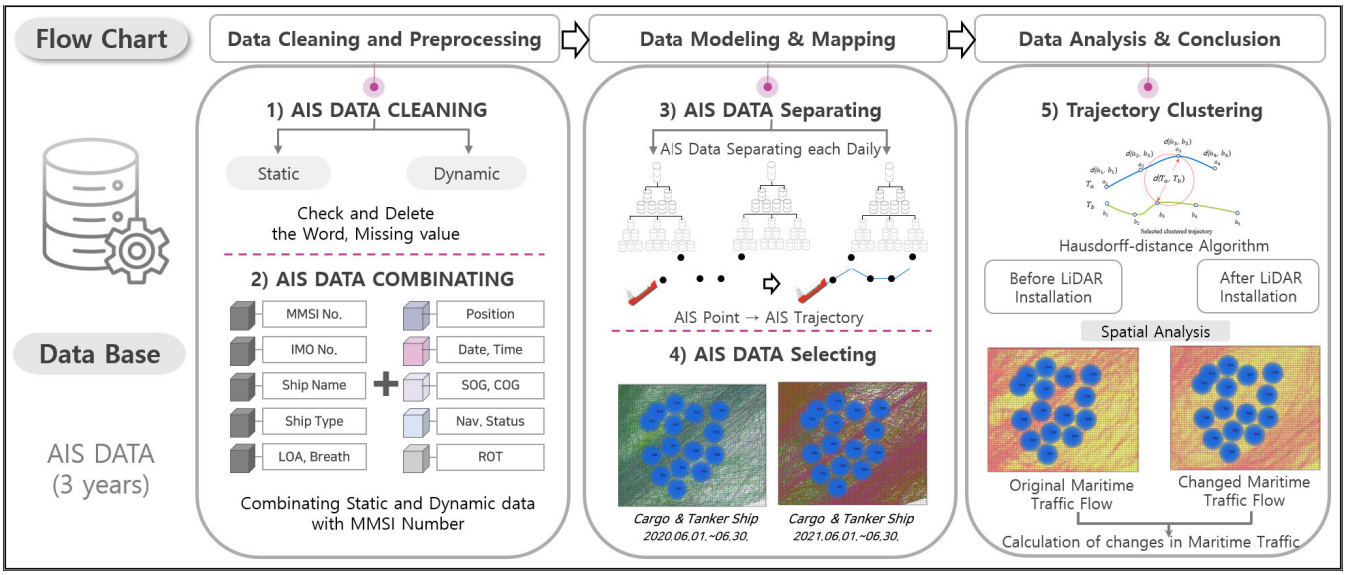

FIGURE 1. Flow chart of changes in maritime traffic patterns.

B. ANALYSIS AREA MODELING

In order to understand the change in maritime traffic patterns, the ocean area where LiDAR are installed in Korea was targeted. The spatial range is latitude 35.12N ∼ 35.63N, longitude 129.84E ∼ 130.60E, and the area is 5,890.73 km^2. The area is located in the exclusive economic zone of Korea. To model the spatial information, the size of the grid is set to 1, and 15 LiDARs included in the space are shown. The positions of each LiDARs were provided to support the research by governmental and wind farm stakeholders. A buffer zone with an interval of 500 m and a radius of up to 5 km was created to effectively visualize the separation distance of ships centered on individual offshore facilities. The minimum boundary including the 5 km buffer zone of these LiDARs indicates a total area of 2,358.68 km^2, confirming a large-scale area, which is expected for the development of offshore wind farm. In this way, the change in maritime traffic patterns is analyzed through spatial modeling. Modeling of the analysis area was created in ArcGIS Pro version 3.0.2, and all information was generated for this study. The modeling of the analysis area is shown in Figure 2.

The appearance of the LiDAR devices installed in this ocean area is shown in Figure 3. Offshore wind farms are planned to be installed in a floating format in this area. Moreover, a total of 15 LiDAR installed between 2020 and 2021 for measuring wind resources, and if future development is approved, the installation of offshore wind turbines is anticipated.

C. ANALYSIS DATA MODELING

To analyze the changes in maritime traffic patterns according to the installation of floating LiDAR, a process of modeling the data to be utilized is performed. The maritime traffic data used for analysis is based on AIS. The AIS data is divided into static information and dynamic information. Static information includes ship type, ship length, ship width, draft and tonnage. Dynamic information includes information such as date, location, speed, course.

Here, a process of pre-processing to use ship AIS data by combining static information and dynamic information is included. In order to select AIS data for analysis, potential impacts can be considered as follows:

1) COVID-19 was declared a pandemic by the World Health Organization (WHO) from January 2020 to May 2023. Maritime traffic data could be influenced by global issues [33]. Therefore, to explore a wide range of data, one-month periods in December 2019, June 2020, December 2020, and June 2021 were selected for analysis.

2) Maritime traffic patterns can be disrupted due to major maritime accidents or other reasons, resulting in vessels halting operations or using alternative routes. For instance, the grounding incident of the EVER GIVEN vessel in the Suez Canal occurred from March 23, 2021, to March 30, 2021. This incident caused a disruption in maritime logistics connecting Europe and Asia, causing changes in the flow of maritime traffic [34]. Therefore, this specific period was excluded from the data analysis.

3) Generally, vessels deviate to avoid adverse weather conditions, such as typhoons. Therefore, it is important to consider whether navigation warnings were in effect during the analysis period. The provided data for December 2019, June 2020, December 2020, and June 2021 were confirmed to be less affected by weather conditions, obtained from government weather agencies.

4) Maritime traffic patterns are influenced by the installation of Floating LiDAR. In the analysis area, a total of 15 LiDAR installations were conducted from October 2020 to April 2021. Each LiDAR was installed differently based on the circumstances and conditions of the developer and operator.

TABLE 1. Changes in ship's type point data according duration.

Ship's Type	AIS point data duration			
	2019.12.01. ~ 2019.12.31.	2020.06.01. ~ 2020.06.30.	2020.12.01. ~ 2020.12.31	2021.06.01. ~ 2021.06.30.
Cargo Ship	743,664	1,192,493	698,079	808,099
Tanker Ship	344,633	485,446	263,283	205,594
Passenger Ship	0	4,906	4,264	6,256
Towing Ship	7,162	135,975	110,122	182,223
Fishing	1,035,095	518,129	1,035,731	585,750
Other Ship	2,012,932	2,019,110	1,546,580	2,301,778
Total	4,143,486	4,356,059	3,658,059	4,089,700

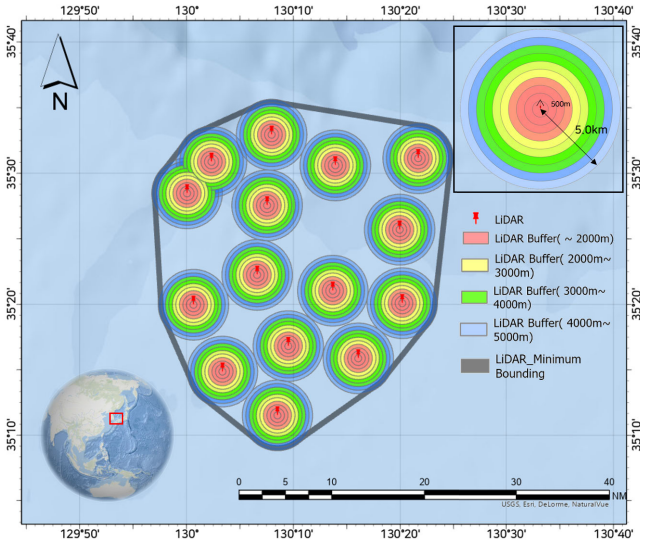

FIGURE 2. Analysis area modeling with LiDAR position.

FIGURE 3. The appearance of LiDAR devices installed in March 2021.

By analyzing various factors such as global issues, maritime accidents, and weather conditions that can impact maritime traffic, a more accurate data analysis can be conducted.

As a result of extracting the AIS data of the analysis area, it is composed of the data shown in Table 1. According to Tsuji's research, it is recommended to analyze maritime traffic data for a period of 6 to 7 days. However, in this study, a total of 4 months of AIS data were utilized [35]. Table 1 shows the duration of AIS point data for different ship types during specific time periods. The AIS point data durations correspond to the periods of December 1, 2019, to December 31, 2019; June 1, 2020, to June 30, 2020; December 1, 2020, to December 31, 2020; and June 1, 2021, to June 30, 2021.

The duration of AIS point data for Cargo Ships was 743,664 points in December 2019, 1,192,493 points in June 2020, 698,079 points in December 2020, and 808,099 points in June 2021. Tanker Ships had AIS point data durations of 344,633 points in December 2019, 485,446 points in June 2020, 263,283 points in December 2020, and 205,594 points in June 2021. There were no Passenger Ships with available AIS point data in December 2019. However, in June 2020, there were 4,906 points of data, followed by 4,264 points in December 2020, and 6,256 points in June 2021. Towing Ships had AIS point data durations of 7,162 points in December 2019, 135,975 points in June 2020, 110,122 points in December 2020, and 182,223 points in June 2021. The duration of AIS point data for Fishing vessels was 1,035,095 points in December 2019, 518,129 points in June 2020, 1,035,731 points in December 2020, and 585,750 points in June 2021. Other ship types had AIS point data durations of 2,012,932 points in December 2019, 2,019,110 points in June 2020, 1,546,580 points in December 2020, and 2,301,778 points in June 2021.

During this analysis, AIS data for various types of vessels was explored over an extended period. To determine the final data analysis period, potential factors that could have influenced maritime traffic were considered. The data from December 2019, which did not fall within the timeframe of the COVID-19 pandemic, was excluded. Additionally, the data from December 2020, when the installation of floating LiDAR was taking place, was also excluded. Maritime traffic data is extracted by dividing before and after the installation of floating LiDARs. The before-installation period of Floating LiDAR was from June 1, 2020, to June 30, 2020, lasting 30 days. The after-installation period occurred one year later, from June 1, 2021, to June 30, 2021.

Table 2 shows the changes in maritime traffic before and after the installation of floating LiDARs, categorized by ship length. The data is divided into four length categories: L1 (less than 100m), L2 (100m to less than 200m), L3 (200m to less than 300m), and L4 (300m or more). The number of ships in each category is compared between the period before installation and the period after installation.

TABLE 2. Changes in ship's length point data according installation.

Ship's Length	Before installation (20.06.01. ~ 06.30.)	After installation (21.06.01. ~ 06.30.)
L1(< 100m)	2,863,985	3,171,414
L2(100m ≤, <200m)	857,448	454,179
L3(200m ≤, < 300m)	415,298	303,835
L4(300m ≤)	219,328	160,272
Total	4,356,059	4,089,700

In the L1 category, there was an increase in the number of ships from 2,863,985 before installation to 3,171,414 after installation. In contrast, the L2 category experienced a decrease in ship numbers from 857,448 before installation to 454,179 after installation. Similarly, the L3 category saw a reduction from 415,298 before installation to 303,835 after installation. Lastly, the L4 category also showed a decrease in ship numbers from 219,328 before installation to 160,272 after installation. In total, there were 4,356,059 ships before installation and 4,089,700 ships after installation. As a result of analyzing the maritime traffic data by length unit of 100m, it was determined that ships shorter than 100m increased, and all ships longer than 100m decreased. As a result of analyzing the type of ship and the length of the ship, it was confirmed that a small ship for the protection of the facility near the installation of the marine facility was newly added. For efficient analysis of the relevant sea area, ships with regular navigation patterns are extracted. For that reason, small ships, fishing boats, and other ships have irregular maritime traffic patterns depending on the purpose of operation. Therefore, the data of cargo ships and tankers are extracted, and the analysis is performed by dividing the ship length into units of 100 m.

D. SPATIAL ANALYSIS MODELING

Spatial analysis is a comprehensive approach used in various fields, such as geography, urban planning, environmental science, and transportation, to study and understand complex spatial relationships, patterns, and processes within data [36]. It involves the examination of spatial data, including geographical locations, attributes, and features, to identify and quantify spatial patterns, correlations, and trends [37]. By employing various quantitative methods, analytical tools, and geographical information system (GIS) techniques, spatial analysis helps researchers and decision-makers make informed decisions based on the spatial characteristics of the data [38]. When the maritime traffic point data of the 30-day analysis period is visualized as a track map, there is a limit to quantitative analysis due to the overlapping of the track results of a large number of ships. In particular, some tracks have errors in AIS time data, and it is difficult to measure changes in maritime traffic patterns due to ship turning [29]. Therefore, the Hausdorff-distance algorithm aims at clustering that connects similar ships and their tracks to each other. This algorithm is also used as the algorithm used to build maritime transportation networks in

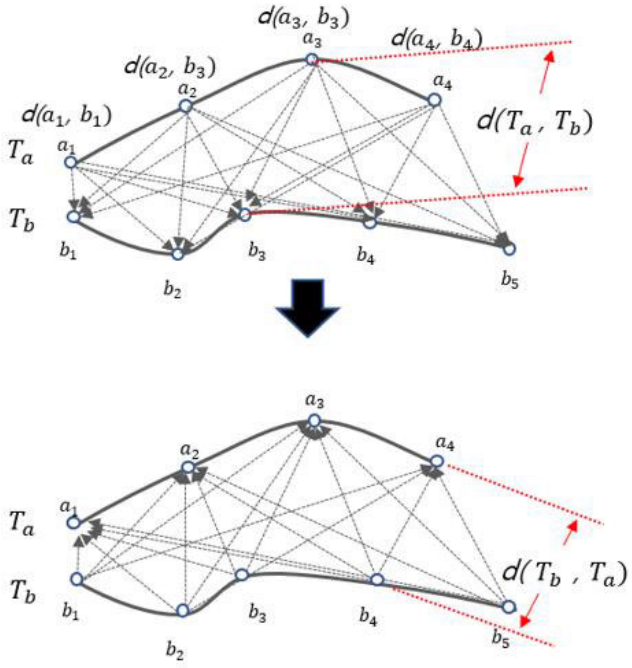

FIGURE 4. Overview of Hausdorff-distance algorithm.

Europe [20]. In general, in the case of commercial ships, economic and safety factors are combined and operated according to the destination port, and the route created is made into a customary route. At this time, it is efficient to reduce data by clustering more similar tracks. Figure 4 shows the concept of the Hausdorff-distance algorithm [20], [39]. This method can represent similar tracks as a matrix and expresses the degree of similarity between individual tracks numerically.

If the Hausdorff–distance is a subset of a non-empty metric space, where T_a represents trajectory a, and T_b represents trajectory b, $d_H(T_a, T_b)$ in the Hausdorff space is expressed as follows.

$$d_H(T_a, T_b) = \max\{d(T_a, T_b), d(T_b, T_a)\} \tag{1}$$

here, T denotes the trajectory, $T_a = [a_1, a_2, \cdots, a_{n-1}, a_n]$ denotes the trajectory of ship a, and $T_b = [b_1, b_2, \cdots, b_{n-1}, b_n]$ denotes the trajectory of ship b. Given two sets of points T_a and T_b, the Hausdorff–distance in one direction is obtained as follows.

$$d(T_a, T_b) = \max\{\min\{\|a_i - b_j\|\}\} \tag{2}$$
$$d(T_b, T_a) = \max\{\min\{\|b_j - a_i\|\}\} \tag{3}$$

here, $\|a_i - b_j\|$ and $\|b_j - a_i\|$ use the Euclidean–distance to define two trajectory points as the Hausdorff–distance. An example of the Hausdorff–distance based on the ship trajectory is shown in Figure 4. Figure 4 shows that the shortest distance from T_a to T_b is $d(a_3, b_3)$, and the shortest distance from T_b to T_a is $d(b_4, a_4)$. In other words, the Hausdorff–distance calculates the largest distance among all

TABLE 3. Classification AIS data to analyze changes in maritime traffic patterns (maritime traffic volume count).

Classification of AIS data analysis	Ship's Type	Ship's Length				Total
		L1 (< 100m)	L2 (100m ≤, <200m)	L3 (200m ≤, < 300m)	L4 (300m ≤)	
Before installation (20.06.01. ~ 06.30.)	Cargo ship and Tanker ship	148	507	317	146	1,118
After installation (21.06.01. ~ 06.30.)	Cargo ship and Tanker ship	129	387	347	136	999
Hausdorff-distance (21.06.01. ~ 06.30.)	Cargo ship and Tanker ship	58	240	309	106	713
Total		335	1,134	973	388	2,830

distances from a point on one trajectory to the nearest point on another trajectory.

III. RESULTS

A. AIS DATA PROCESING RESULT

In order to analyze changes in maritime traffic patterns, the process of segmenting AIS data included in the spatial range is performed. Here, cargo ships and tankers that show regular maritime traffic patterns are the targets. Small ships, fishing boats, and other ships show irregular operation patterns due to the characteristics of ships, so they are excluded from the traffic patterns analysis. Table 3 shows the data changes of cargo ships and tankers before and after the installation of LiDARs, and the changes in track data clustered with the Hausdorff-distance algorithm. Analyze the global maritime traffic patterns before and after the installation of LiDARs, and analyze the local maritime traffic patterns according to Hausdorff-distance clustering. Table 3 presents the classification of AIS data used to analyze changes in maritime traffic patterns. The data is classified based on ship type and ship length, with four length categories (L1: $<$ 100m, L2: 100m $\leq$, $<$ 200m, L3: 200m $\leq$, $<$ 300m, L4: 300m $\leq$). The table shows the maritime traffic volume count for cargo and tanker ships before and after the installation of LiDARs, as well as the count after using the Hausdorff-distance algorithm to analyze the data. Before installation, there were a total of 1,118 ships, with 148 in L1, 507 in L2, 317 in L3, and 146 in L4.

After installation, the total number of ships decreased to 999, with 129 in L1, 387 in L2, 347 in L3, and 136 in L4. After using the Hausdorff-distance algorithm, the total count decreased to 713, with 58 in L1, 240 in L2, 309 in L3, and 106 in L4. Overall, there were 335 ships in L1, 1,134 in L2, 973 in L3, and 388 in L4, resulting in a total of 2,830 ships analyzed.

B. SPATIAL ANALYSIS RESULT

AIS data is basically composed of points. If connected in chronological order based on MMSI (Maritime Mobile Service Identity), the track chart of the ship can be displayed. First of all, the process of expressing the data by length generated based on the cargo ship and tanker ship in the form of a layer is performed. Changes in maritime traffic according to the installation of LiDARs can be confirmed through the track chart. Also, from the Hausdorff-distance clustering, the process of compressing and reducing the trace diagram to a similar one is performed.

Generated with a size of 1 km. Each track chart is analyzed as a traversal spinal cord by counting the track charts included in the cell. The results of spatial analysis based on maritime traffic data are shown in Figure 5. Figure 5 is an effective method for visualizing changes in maritime traffic patterns before and after the installation of LiDARs. Using this method, it is possible to determine the direction of traffic patterns changes. AIS point data was converted into trajectory lines for each vessel and summarized within 1km grids to calculate the number of vessels passing through. This function overlays a grid layer on top of another layer in order to generate a summary of line counts, line lengths within each grid. It also calculates statistical attributes of the features within the grids.

C. CHANGES IN GLOBAL MARITIME TRAFFIC PATTERNS

The area near Korea, which is the analysis space in this study, is an integrated floating LiDAR complex with a total area of 2,358.68 km^2 and a circumference of 148 km. This measurement value is one large area created based on the value of keeping the boundary line of radius 5km of each. Therefore, we want to analyze how the overall patterns of maritime traffic changes in one large area. This analysis shows the values that change before and after the installation of LiDARs. Figure 6(a) shows the results of the global traffic patterns before the installation of LiDARs. The patterns are based on cargo ships and tankers for the month of June 2020, and it is analyzed that maritime traffic is concentrated diagonally in the analysis space. The gate line of 109 km length was created in the center of the analysis area and divided into three parts to analyze the number of traffic vessels. As a result, the center maritime traffic route was formed. The analysis after installation of LiDARs is shown in Figure 6(b), targeting cargo ships and tankers for the month of June 2021. It can be seen that the central maritime traffic patterns divided into three maritime traffic patterns.

The North Maritime Traffic Route and the South Maritime Traffic Route of the agglomeration complex were created, and the spatial scope of the central maritime traffic patterns was reduced. The global maritime traffic patterns moved 12 km from the center to the north and south, and the change is shown in Table 4.

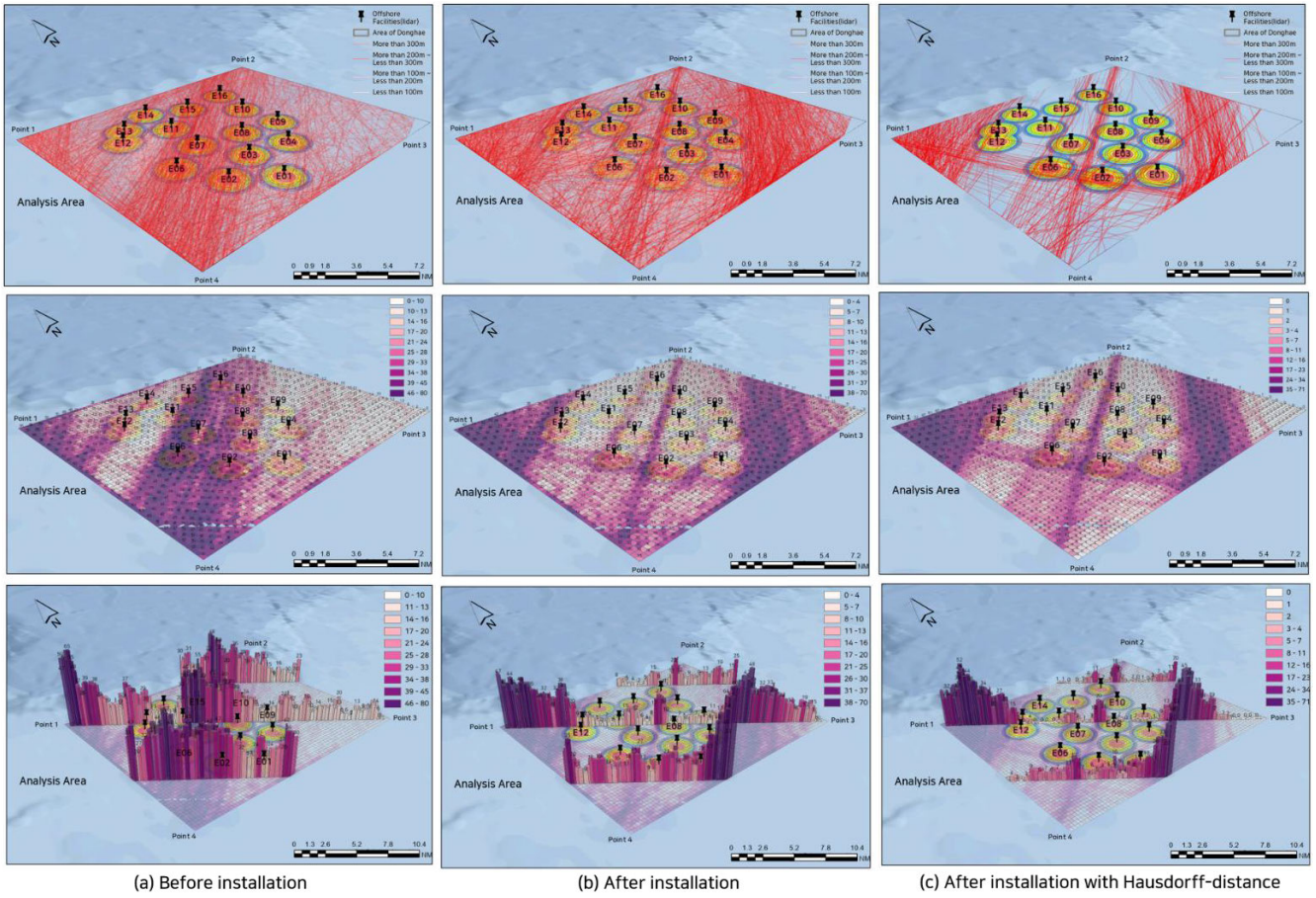

FIGURE 5. Visualization of maritime traffic patterns through spatial analysis, (a) Before installation LiDAR (b) After installation LiDAR (c) Before installation LiDAR with Hausdorff-distance.

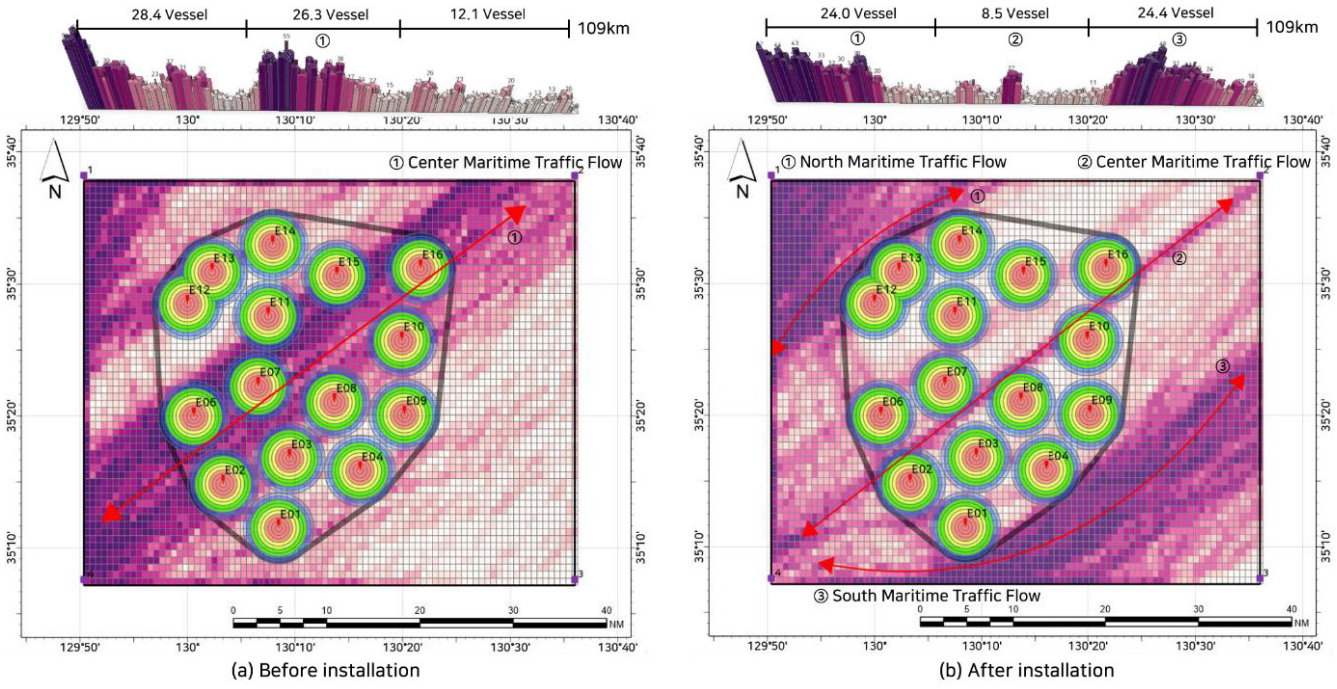

FIGURE 6. Globally maritime traffic patterns (a) Before installation of marine facilities (b) After installation of marine facilities.

TABLE 4. Separate AIS to analyze changes in maritime traffic patterns.

Gate line (109km)	Before (Avg./gate line)	After (Avg./gate line)	Rate of change
North	28.4	24.0	- 4.4
Center	26.3	8.5	- 17.8
South	12.1	24.4	+ 12.3

This table shows the results of separating AIS data to analyze changes in maritime traffic patterns based on three gate lines (109km). In order to analyze changes in maritime traffic patterns, the average of ships passing through the northern, central, and southern gate lines was analyzed in 30 days. The gate line in the North had an average of 28.4 vessels passing through before the installation and 24.0 vessels passing through after the installation. The central gate line had an average of 26.3 vessels passing through before the installation and 8.5 vessels passing through after the installation. The southern gate line had an average of 12.1 vessels passing through before the installation and 24.4 vessels passing through after the installation. These results suggest that the installation of LiDARs had a varying impact on maritime traffic patterns, with significant decreases in traffic observed in the central gate line, while an increase in traffic was observed in the southern gate line. As a result, after the installation of LiDARs, the northern maritime traffic decreased by an average of 4.4 vessels, and the central maritime traffic decreased by an average of 17.8 vessels. Meanwhile, the southern maritime traffic increased by an average of 12.3 vessels.

D. CHANGES IN LOCAL MARITIME TRAFFIC PATTERNS

As a result of the global analysis according to the aggregation complex of LiDARs, the maritime traffic patterns changed into north, central, and south maritime traffic patterns as a whole. As a peculiarity, some vessels maintain a slight central maritime traffic pattern. This Figure 7 shows the analysis of the local maritime traffic patterns revealed that different navigation patterns exist depending on the length of the ships. The navigation pattern for L1 shows that traffic is concentrated around the LiDAR positions E01, E02, and E06. Similarly, the navigation pattern for L2 indicates that ships mainly operate around the LiDAR positions E01, E02, E03, E04, E06, E12, and E13. For relatively larger ships such as L3 and L4, the maritime traffic pattern is in a northeast-southwest route. It can also be seen that larger buffer zones are formed from the central position of the LiDAR. Therefore, the closest distances between each ship trajectory within the 5km buffer zone of the LiDAR were measured, and the results are shown in Table 5. This Table 5 shows the nearest buffer distance of ships from each LiDAR position categorized by ship's length (L1: $<$100m, L2: 100m$\leq$, $<$200m, L3: 200m$\leq$, $<$300m, L4: 300m$\leq$). The minimum distance of the table shows the nearest buffer distance observed for each ship length category (L1 to L4) at each LiDAR location. For example, the minimum buffer distance for L2 ships at E06 LiDAR was 125.75 meters. The maximum distance shows the largest buffer distance observed for each ship length category at each LiDAR location. The maximum buffer distance observed was 4,987.97 meters for L2 ships at E10 LiDAR.

For instance, the SD for L2 ships was the highest among all ship length categories. The average distance shows the mean buffer distance for each ship length category at each LiDAR location. For L1 ships (less than 100m in length) was 1,382.92 meters.

Similarly, the average distance LiDAR to L2 ships (between 100m and 200m in length) was 1,738.78 meters, while for L3 ships (between 200m and 300m in length), it was 2,467.36 meters, and for L4 ships (more than 300m in length), it was 1,996.81 meters. This study analyzed the distance at which maritime traffic patterns change according to the length of ships. As previously explained, various methods were used to calculate a safe buffer zone, and the standards for these calculations were not clearly defined. This research proposes a safe buffer zone for navigation between marine facilities, such as LiDAR, and ships, considering the specific characteristics of different types of vessels. Therefore, considering the maritime environment, buffer distances of ships taking into consideration safety measures would be helpful in promoting safe ship operations and preventing maritime accidents.

IV. DISCUSSION

Ships serve as an efficient means of utilizing the vast ocean space to transport the world's cargo. Over time, shipping routes have been developed and established as economical and safety-efficient, reflecting conventional navigation patterns. In recent years, the development of renewable energy has been actively pursued in response to climate change, expanding from the spatially limited land to the ocean. In particular, offshore wind farms are emerging as major users of large-scale marine space, leading to increased friction with maritime traffic. While this paper acknowledges the importance of maintaining shipping routes, it also recognizes the need for coexistence with the development of offshore wind farms. Therefore, conducted a study on the changes in maritime traffic patterns due to the installation of LiDARs. Table 6 presents the results of average distance divided by ship length categories. The average distance for each length category is calculated and compared to the maximum ship's length within the respective category.

The ratios of distance to maximum length are found to be 13.96L for L1, 8.73L for L2, 8.25L for L3, and 6.65L for L4. This table provides insights into how the average distance varies across different ship length categories. These results show the changes in maritime traffic patterns depending on the length of the ships. On average, all ships form a buffer zone of more than 6L when navigating. However, this distance does not indicate whether the ships navigated on the starboard side or the port side of the LiDAR. Meanwhile,

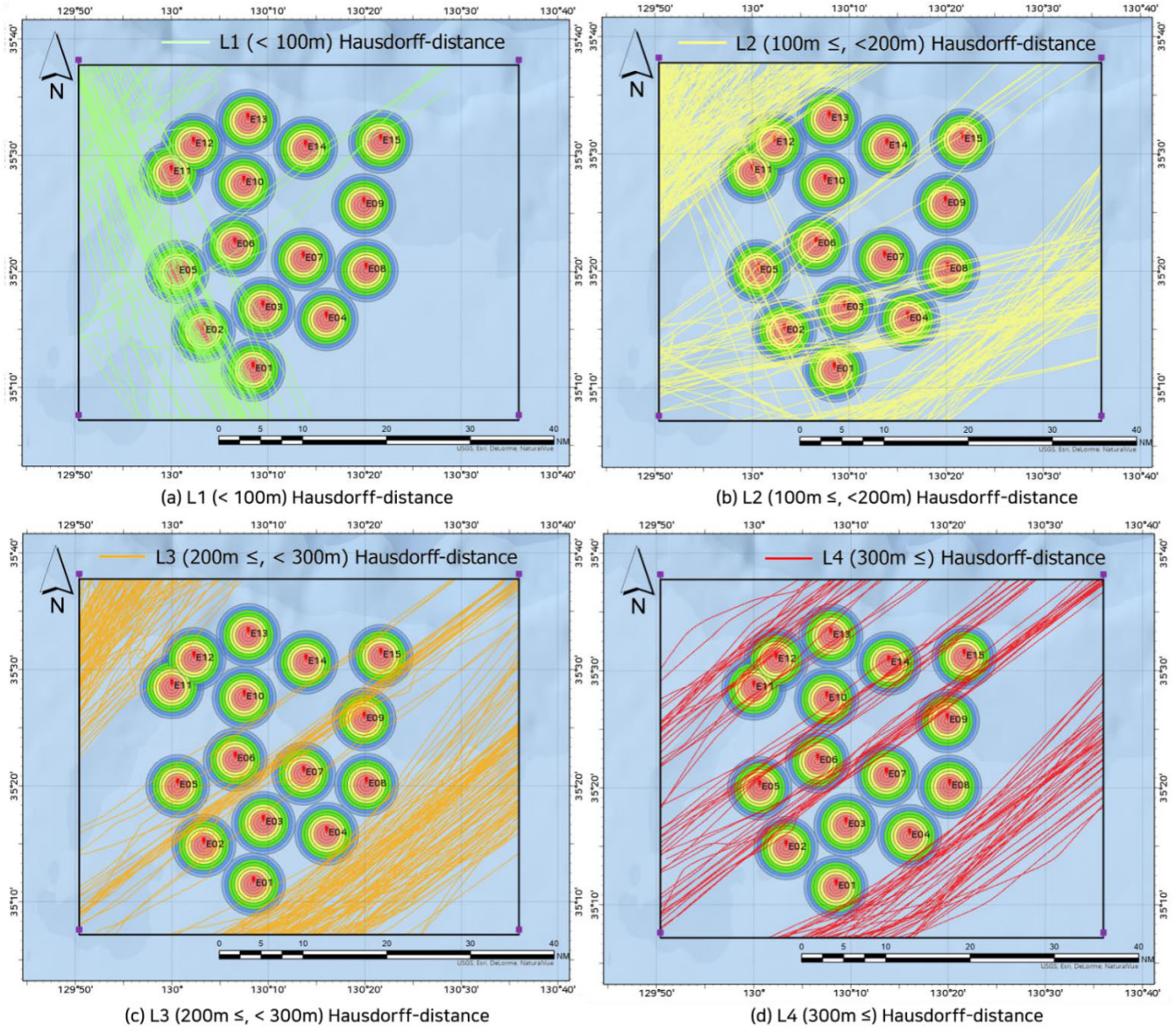

FIGURE 7. Locally maritime traffic patterns with Hausdorff-distance, (a) trajectory line of L1 (< 100m) (b) trajectory line of L2 (100m ≤, < 200m) (c) trajectory line of L3 (200m ≤, < 300m) (d) trajectory line of L4 (300m ≤).

according to PIANC WG 161, the buffer zone between maritime traffic and offshore wind farm facilities is proposed as follows [6]. If the offshore wind farm is installed on the starboard side of the ship, it follows Equation 4, and if it is installed on the port side of the ship, it follows Equation 5.

$$Starboard\ side = 6L + 500m + 0.3NM \quad (4)$$

$$Port\ side = 6L + 500m \quad (5)$$

The turning performance of ships varies depending on the starboard side and the port side. Here, L represents the length of the ship, which is generally applied to the maximum ship size that sails through the area where an offshore wind farm is planned for development. Additionally, NM (1 Nautical Mile = 1,852m) is represented and added separately for the starboard side. Therefore, by applying the PIANC guidelines, the maritime traffic patterns were compared for both the starboard side and the port side. Figure 8 shows the maritime traffic patterns of ships navigating through offshore wind farms and buffer zones according to the PIANC guidelines.

In the case of ship size L1, the analysis showed a difference of −272.62m for PIANC's starboard and +282.98m for the port. For L2, the difference was −516.76m for starboard and +38.84m for the port. In L3, the difference was −388.18m for starboard and +167.42m for the port. In L4, both starboard and port showed lower values, with −1,458.73m and −903.13m, respectively. For L1 to L3, the changed maritime traffic patterns did not satisfy PIANC's starboard criteria but met the port criteria. On the other hand, L4 had a very large ship size, so PIANC's criteria appeared relatively high, and the changed maritime traffic patterns did not meet

TABLE 5. Nearest buffer distance from LiDAR by ship's length.

Position of LiDAR	Nearest buffer distance from LiDAR by Ship's Length			
	L1	L2	L3	L4
E01	1,114.83 m	972.52 m	2,060.45 m	3,735.57 m
E02	445.24 m	783.33 m	1,131.78 m	2,194.55 m
E03	1,115.12 m	732.63 m	1,647.90 m	-
E04	-	752.71 m	3,592.79 m	3,712.01 m
E05	138.18 m	508.22 m	891.38 m	1,436.16 m
E06	1,103.49 m	125.75 m	3,245.04 m	2,739.36 m
E07	-	3,850.99 m	1,207.35 m	3,587.77 m
E08	-	483.52 m	4,542.09 m	-
E09	-	3,024.68 m	1,360.72 m	1,862.10 m
E10	3,649.58 m	4,987.97 m	4,300.66 m	859.79 m
E11	1,259.13 m	569.23 m	2,215.70 m	964.10 m
E12	1,814.56 m	795.94 m	2,091.84 m	1,051.25 m
E13	-	3,286.61 m	-	1,025.95 m
E14	1,704.21 m	4,300.05 m	3,657.94 m	839.17 m
E15	1,484.88 m	907.58 m	2,597.45 m	1,950.77 m
Min. distance	445.24 m	125.75 m	891.38 m	839.17 m
Max. distance	3,649.58 m	4,987.97 m	4,542.09 m	3,735.57 m
SD	948.87 m	1,642.13 m	1,211.88 m	1,116.45 m
Average distance	1,382.92 m	1,738.78 m	2,467.36 m	1,996.81 m

TABLE 6. Results of average distance divided by ship length categories.

Length Categories (Max. Length)	L1 (< 100m)	L2 (100m ≤, <200m)	L3 (200m ≤, <300m)	L4 (300m ≤)
Average Distance	1,382.92m	1,738.78m	2,467.36m	1,996.81m
Max. Length	99.9m	199.9m	299.9m	399.9m
Distance / Max. Length	13.96L	8.73L	8.25L	6.65L

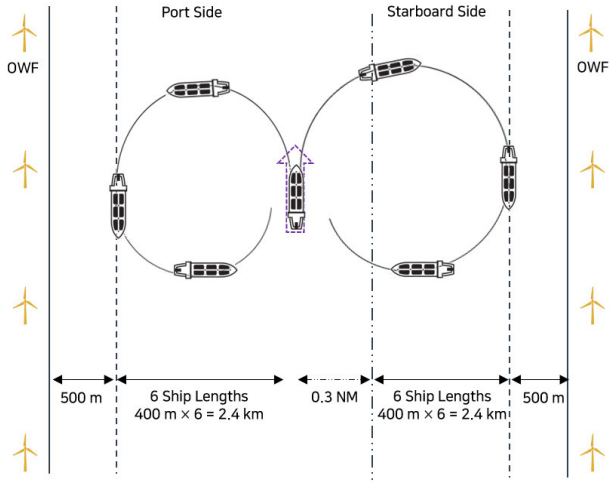

FIGURE 8. Comparison of PIANC guidelines and changes in maritime traffic patterns.

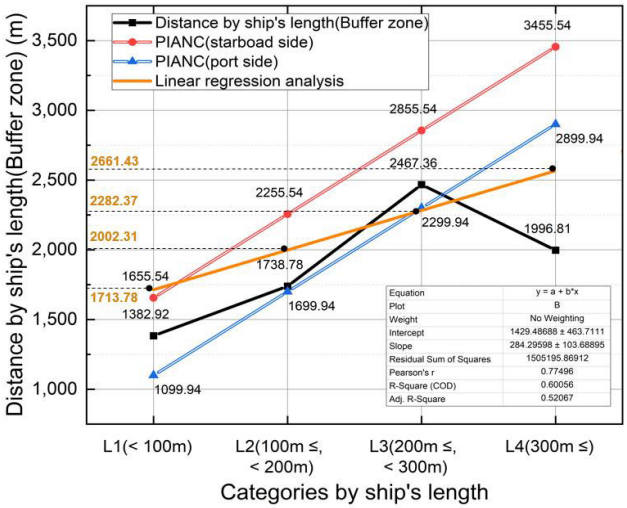

FIGURE 9. Determining buffer zones by ship's length using linear regression.

the criteria. In this study, we aimed to derive a suitable model through linear regression analysis by analyzing the changed pattern distances for each ship length based on the installed LiDAR. To increase the number of dependent variables, the ship length categories were divided into 50m increments instead of 100m increments and calculated in the same way. Ultimately, the results of the linear regression analysis were analyzed as shown in Figure 9. This equation and statistical summary represent the results of a linear regression analysis examining the relationship between ship length x and buffer zone y. The equation is in the form of $y = a + bx$. The intercept a is 1429.48m, with a standard error of 463.71m, and the slope b is 284.29m, with a standard error of 103.68m.

The aim is to supplement PIANC guidelines and enable a diverse range of approaches. The methodology employed in this study shows promise in forecasting changes in maritime traffic patterns. This indicates that as the ship's length increases, buffer zone distance also increases.

The Pearson's r, which measures the strength and direction of the linear relationship between two variables, is 0.77. This value suggests a strong positive correlation between the ship's length and the buffer zone distance. The R-Square (Coefficient of Determination, COD) is 0.6005, which means that 60.05% of the variation in the buffer zone distance can be explained by the ship's length. The Adjusted R-Square, which adjusts the R-Square for the number of predictor variables and the sample size, is 0.5206. This indicates that the model's explanatory power is relatively high when considering the complexity of the model and the available data. Overall, this analysis shows a significant positive relationship between a ship's length and the buffer zone distance, with the model explaining a considerable portion of the variation in the data. Therefore, the final buffer zones derived from this study were determined to be 1,713.78m for L1, 2,002.31m for L2, 2,282.37m for L3, and 2,661.43m for L4. Each of these criteria includes a margin of error, and they offer scalability that allows for their application in conjunction with various other standards.

The implications and discussion points derived from this study are as follows:

1) The installation of marine facilities such as LiDAR has a significant impact on maritime traffic patterns. Therefore, spatial analysis and the Hausdorff-distance algorithm were utilized to analyze the buffer zone between ships and marine facilities. In particular, the buffer zone derived varies depending on the length of the ship, with longer ships requiring a larger buffer zone.

2) The standards for calculating the buffer zone between maritime traffic and marine facilities are differentiated by the starboard side and port side of the ship, as described by PIANC. These standards are based on the ship's maneuverability and experience. In this study, a new linear regression equation was calculated using AIS data collected over a month. As a result, the significance was secured, and the possibility of calculating a new buffer zone was obtained.

3) Securing a sufficient buffer zone distance is an essential prerequisite for preventing marine accidents. However, the marine environment not only involves maritime traffic but also necessitates coexistence with other marine activities such as renewable energy.

On the other hand, the limitations and future research directions of this study are as follows: The ship lengths were divided into 100m units and analyzed as L1, L2, L3, and L4. There is a need to analyze the distance between ships and marine facilities in more detail by further dividing the ship lengths. Additionally, the aim is to secure a large number of independent variables for future linear regression analysis, in order to achieve a high R-Square value. Moreover, the limitation of this study lies in differentiating the types of ships into cargo ships and tankers only. If various types of ships are added to the analysis, the research results are expected to yield new insights. Maritime traffic patterns can be significantly influenced by global issues. Recent events such as pandemics and canal accidents have demonstrated the potential for changes in maritime traffic. Therefore, there is a need for maritime traffic pattern analysis that considers the complexities of the maritime environment.

V. CONCLUSION

This study provides valuable insights into analyzing the impact of floating LiDAR installations on maritime traffic patterns, utilizing spatial analysis techniques. Marine facilities can significantly affect the navigation patterns of ships, making it crucial to examine changes in maritime traffic. By analyzing buffer zone data for 15 LiDAR systems installed at sea and ships navigating the area, this study offers a basis for predicting changes in maritime traffic patterns and suggesting quantitative modifications for marine facility installations. Moreover, the presented methodology for calculating the new buffer zone serves as a valuable resource for deducing changes in maritime traffic patterns, ensuring safe maritime traffic in complex marine environments and promoting sustainable development. The study is of utmost significance in understanding the impact of marine facilities on maritime traffic patterns and their potential implications on safe and efficient shipping.

REFERENCES

[1] E. Tu, G. Zhang, L. Rachmawati, E. Rajabally, and G.-B. Huang, "Exploiting AIS data for intelligent maritime navigation: A comprehensive survey from data to methodology," *IEEE Trans. Intell. Transp. Syst.*, vol. 19, no. 5, pp. 1559–1582, May 2018.

[2] H.-T. Lee, H.-M. Choi, J.-S. Lee, H. Yang, and I.-S. Cho, "Generation of Ship's passage plan using data-driven shortest path algorithms," *IEEE Access*, vol. 10, pp. 126217–126231, 2022.

[3] J.-S. Lee, W.-J. Son, H.-T. Lee, and I.-S. Cho, "Verification of novel maritime route extraction using kernel density estimation analysis with automatic identification system data," *J. Mar. Sci. Eng.*, vol. 8, no. 5, p. 375, May 2020.

[4] J. Weng and D. Yang, "Investigation of shipping accident injury severity and mortality," *Accident Anal. Prevention*, vol. 76, pp. 92–101, Mar. 2015.

[5] *United Nations Convention on the Law of the Sea*, United Nations, New York, NY, USA, 1982, p. 45, vol. 60.

[6] *WG 161 Interaction Between Offshore Wind Farms and Maritime Navigation*, PIANC, Brussels, Belgium, 2018, pp. 15–16.

[7] *MGM 543 Safety of Navigation Offshore Renewable Energy Installations (OREIs) Guidance on U.K. Navigational Practice, Safety and Emergency Response*, UK MCA, London, U.K. 2016, p. 18.

[8] F. Douvere, "The importance of marine spatial planning in advancing ecosystem-based sea use management," *Mar. Policy*, vol. 32, no. 5, pp. 762–771, Sep. 2008.

[9] M. A. Al-Quhali, M. Baldauf, and M. Fiorini, "Enhanced maritime spatial planning through VTS," in *Proc. 16th Int. Conf. Intell. Transp. Syst. Telecommun. (ITST)*, Oct. 2018, pp. 1–5.

[10] M. Ntona and E. Morgera, "Connecting SDG 14 with the other sustainable development goals through marine spatial planning," *Mar. Policy*, vol. 93, pp. 214–222, Jul. 2017.

[11] J. Chen, C. Claramunt, E. Saux, P. Peng, Q. Mei, and Y. Suo, "Present status and challenges for the interaction between offshore wind farms and maritime navigation in the Taiwan strait," in *Proc. Offshore Energy Storage Summit (OSES)*, Jul. 2019, pp. 1–3.

[12] J.-S. Lee and I.-S. Cho, "Extracting the maritime traffic route in Korea based on probabilistic approach using automatic identification system big data," *Appl. Sci.*, vol. 12, no. 2, p. 635, Jan. 2022.

[13] M. A. Mohandes and S. Rehman, "Wind speed extrapolation using machine learning methods and LiDAR measurements," *IEEE Access*, vol. 6, pp. 77634–77642, 2018.

[14] C. B. Moorthy, M. K. Deshmukh, and D. Mukherejee, "Optimal location of wind turbines in a wind farm using genetic algorithm," *TELKOMNIKA Indonesian J. Electr. Eng.*, vol. 12, no. 8, pp. 658–665, Aug. 2014.

[15] S. A. Breithaupt, M. Bensi, and A. Copping, "AIS-based characterization of navigation conflicts along the U.S. Atlantic coast prior to development of wind energy," *Ocean Eng.*, vol. 264, Nov. 2022, Art. no. 112235.
[16] W. Hasbi, "Tracking capability and detection probability assessment of space-based automatic identification system (AIS) from equatorial and polar orbiting satellites constellation," *IEEE Access*, vol. 8, pp. 184120–184136, 2020.
[17] Z. Yan, Y. Xiao, L. Cheng, R. He, X. Ruan, X. Zhou, M. Li, and R. Bin, "Exploring AIS data for intelligent maritime routes extraction," *Appl. Ocean Res.*, vol. 101, Aug. 2020, Art. no. 102271.
[18] G. Pallotta, M. Vespe, and K. Bryan, "Vessel pattern knowledge discovery from AIS data: A framework for anomaly detection and route prediction," *Entropy*, vol. 15, no. 12, pp. 2218–2245, Jun. 2013.
[19] W.-J. Son, J.-S. Lee, H.-T. Lee, and I.-S. Cho, "An investigation of the ship safety distance for bridges across waterways based on traffic distribution," *J. Mar. Sci. Eng.*, vol. 8, no. 5, p. 331, May 2020.
[20] V. F. Arguedas, G. Pallotta, and M. Vespe, "Maritime traffic networks: From historical positioning data to unsupervised maritime traffic monitoring," *IEEE Trans. Intell. Transp. Syst.*, vol. 19, no. 3, pp. 722–732, Mar. 2018.
[21] H.-T. Lee, J.-S. Lee, H. Yang, and I.-S. Cho, "An AIS data-driven approach to analyze the pattern of ship trajectories in ports using the DBSCAN algorithm," *Appl. Sci.*, vol. 11, no. 2, p. 799, Jan. 2021.
[22] L. Wang, P. Chen, L. Chen, and J. Mou, "Ship AIS trajectory clustering: An HDBSCAN-based approach," *J. Mar. Sci. Eng.*, vol. 9, no. 6, p. 566, May 2021.
[23] J. Liu, C. Li, J. Bai, Y. Luo, H. Lv, and Z. Lv, "Security in IoT-enabled digital twins of maritime transportation systems," *IEEE Trans. Intell. Transp. Syst.*, vol. 24, no. 2, pp. 2359–2367, Feb. 2023.
[24] J.-E. Giering and A. Dyck, "Maritime digital twin architecture," *At Automatisierungstechnik*, vol. 69, no. 12, pp. 1081–1095, Dec. 2021.
[25] Z. Yan, Y. Xiao, L. Cheng, S. Chen, X. Zhou, X. Ruan, M. Li, R. He, and B. Ran, "Analysis of global marine oil trade based on automatic identification system (AIS) data," *J. Transp. Geography*, vol. 83, Feb. 2020, Art. no. 102637.
[26] W.-J. Son, J.-S. Lee, B.-K. Lee, and I.-S. Cho, "A study on the selection of the recommended safety distance between marine structures and ships based on AIS data," *J. Navigat. Port Res.*, vol. 43, no. 6, pp. 420–428, 2019.
[27] S. Khandker, H. Turtiainen, A. Costin, and T. Hamalainen, "Cybersecurity attacks on software logic and error handling within AIS implementations: A systematic testing of resilience," *IEEE Access*, vol. 10, pp. 29493–29505, 2022.
[28] *Technical Characteristics for an Automatic Identification System Using Time Division Multiple Access in the VHF Maritime Mobile Frequency Band*, document ITU-R M. 1371-5, Radiocommunication Sector of International Telecommunication Union (ITU-R), 2014, p. 114.
[29] J.-S. Lee, H.-T. Lee, and I.-S. Cho, "Maritime traffic route detection framework based on statistical density analysis from AIS data using a clustering algorithm," *IEEE Access*, vol. 10, pp. 23355–23366, 2022.
[30] Y.-J. Kim, J.-S. Lee, G.-Y. Kong, and I.-S. Cho, "A study on the creation of high density depth contours in coastal waters using spatial analysis based on depth and AIS data," *Korea Soc. Coastal Disaster Prevention*, vol. 9, no. 2, pp. 157–165, Apr. 2022.
[31] Y. Zhang and W. Li, "Dynamic maritime traffic pattern recognition with online cleaning, compression, partition, and clustering of AIS data," *Sensors*, vol. 22, no. 16, p. 6307, Aug. 2022.
[32] C.-H. Yang, C.-H. Wu, J.-C. Shao, Y.-C. Wang, and C.-M. Hsieh, "AIS-based intelligent vessel trajectory prediction using bi-LSTM," *IEEE Access*, vol. 10, pp. 24302–24315, 2022.
[33] D. Yazir, B. Sahin, T.-L. Yip., and P.-H. Tseng, "Effects of COVID-19 on maritime industry: A review," *Int. Maritime Health*, vol. 71, no. 4, pp. 253–264, 2020.
[34] S. Fan, Z, Yang, J. Wang, and J. Marsland, "Shipping accident analysis in restricted waters: Lesson from the Suez Cannal blockage in 2021," *Ocean Eng.*, vol. 266, Dec. 2022, Art. no. 113119.
[35] K. Tsuji, "Methods of survey for marine traffic," *Jpn. Inst. Navigat.*, vol. 129, pp. 8–18, Jan. 1996.
[36] J. Monios and A. K. Y. Ng, "Competing institutional logics and institutional erosion in environmental governance of maritime transport," *J. Transp. Geography*, vol. 94, Jun. 2021, Art. no. 103114.
[37] D. Tocchi, C. Sys, A. Papola, F. Tinessa, F. Simonelli, and V. Marzano, "Hypergraph-based centrality metrics for maritime container service networks: A worldwide application," *J. Transp. Geography*, vol. 98, Jan. 2022, Art. no. 103225.
[38] Y.-J. Kim, J.-S. Lee, A. Pititto, L. Falco, M.-S. Lee, K.-K. Yoon, and I.-S. Cho, "Maritime traffic evaluation using spatial–temporal density analysis based on big AIS data," *Appl. Sci.*, vol. 12, no. 21, Nov. 2022, Art. no. 11246.
[39] R. Laxhammar and G. Falkman, "Sequential conformal anomaly detection in trajectories based on Hausdorff distance," in *Proc. 14th Int. Conf. Inf. Fusion*, Jul. 2011, pp. 1–8.

JEONG-SEOK LEE received the B.S. degree from the Division of Navigation Science, Korea Maritime and Ocean University, Busan, South Korea, in 2014. From 2014 to 2017, he was a Navigator for the third and second officers with SK Shipping Company, with experience in bulk carriers, product oil-tanker carriers, and very large crude oil carriers. In 2018, he performed related works as a Maritime Simulator Operator and is currently conducting research using maritime traffic data. He conducted research using maritime data-based computing algorithm. In particular, he uses the GIS program in maritime. His research interest includes fusion research using artificial intelligence techniques.

MOON-SUK LEE received the Ph.D. degree from the Interdisciplinary Program in Science and Technology, Graduate School, Korea University. She is currently the Head of the Ocean Policy Research Center, Korea Institute of Ocean Science and Technology. In particular, she is providing policy support for marine spatial planning in South Korea and working on the development of digital twins for various industrial sectors that utilize marine spaces. Her main research interests include marine spatial planning, marine environmental policy, and coastal management policy.

IK-SOON CHO received the B.Sc. degree in nautical science, in 1996, the M.E. degree in maritime transportation science from Korea Maritime and Ocean University (KMOU), Busan, South Korea, in 2000, and the Ph.D. degree from the Graduate School of Science and Technology, Kobe University, Kobe, Japan, in 2005. He was with the Traffic Safety Audit Center, KMOU, based on the Korea Maritime Safety Act. He is currently a Professor with the Division of Navigation Convergences Studies, College of Maritime Sciences, KMOU. His main research interests include maritime safety evaluation, ship operation, and mooring safety analysis based on big-data using the machine learning and deep learning algorithm.